

# Synthesis of cerium oxide (CeO<sub>2</sub>) by co-precipitation for application as a reference material for X-ray powder diffraction peak widths

Anderson Márcio de Lima Batista,<sup>1,a)</sup> Marcus Aurélio Ribeiro Miranda,<sup>2</sup>

Fátima Itana Chaves Custódio Martins,<sup>3</sup> Cássio Morilla Santos,<sup>2</sup> and José Marcos Sasaki<sup>2</sup>

<sup>1</sup>Departamento de Engenharia Metalúrgica e de Materiais, Centro de Tecnologia, Universidade Federal do Ceará – UFC, 60455-760, Fortaleza, CE, Brazil

<sup>2</sup>Departamento de Física, Centro de Ciências, Universidade Federal do Ceará – UFC, 60440-970, Fortaleza, CE, Brazil

<sup>3</sup>Departamento de Química Analítica e Físico-Química, Centro de Ciências, Universidade Federal do Ceará – UFC, 60455-700, Fortaleza, CE, Brazil

(Received 27 June 2017; accepted 24 October 2017)

Several methods can be used to obtain, from powder diffraction patterns, crystallite size and lattice strain of polycrystalline samples. Some examples are the Scherrer equation, Williamson–Hall plots, Warren/Averbach Fourier decomposition, Whole Powder Pattern Modeling, and Debye function analysis. To apply some of these methods, it is necessary to remove the contribution of the instrument to the widths of the diffraction peaks. Nowadays, one of the main samples used for this purpose is the LaB<sub>6</sub> SRM660b commercialized by the National Institute of Standard Technology; the width of the diffraction peak of this sample is caused only by the instrumental apparatus. However, this sample can be expensive for researchers in developing countries. In this work, the authors present a simple route to obtain micron-sized polycrystalline CeO<sub>2</sub> that have a full width at half maximum comparable with the SRM660b and therefore it can be used to remove instrumental broadening. © 2018 International Centre for Diffraction Data. [doi:10.1017/S0885715617001208]

Key words: X-ray diffraction, standard reference material, cerium oxide, instrumental broadening

## I. INTRODUCTION

The crystallite size and lattice strain are quantities often obtained from X-ray powder diffraction patterns. Several methods can be used to obtain these quantities, such as the Scherrer equation (Patterson, 1939; Azároff and Buerger, 1958; Klug and Alexander, 1974; Langford and Wilson, 1978; Vives *et al.*, 2004; Burton *et al.*, 2009; Holzwarth and Gibson, 2011) Warren/Averbach Fourier decomposition (Warren and Averbach, 1950), Williamson–Hall plot (Hall, 1949; Williamson and Hall, 1953), Whole Powder Pattern Modeling – WPPM (Scardi *et al.*, 2010) and Debye Function Analysis (Cervellino *et al.*, 2015). Among these methods, the Scherrer equation and the Williamson–Hall plot are arguably the easiest to apply which makes them widely used, despite being rough approximations. In the Scherrer equation, the volume averaged crystal size for the column underlying the *hkl* direction depends on the full width at half maximum of the diffraction peak by the following equation:

$$D = \frac{k\lambda}{\beta \cos \theta}, \quad (1)$$

in which  $D$  is the crystallite size,  $\beta$  is the full width at half maximum,  $\lambda$  is the X-ray wavelength,  $\theta$  is the Bragg angle of the reflection under consideration, and  $k$  is a constant related to the shape and symmetry of the crystallite and is approximately 1 for a spherical crystallite (James, 1962; Langford and

Wilson, 1978). In the Williamson–Hall plot, the width  $\beta$  is treated as a linear combination of the effects of size,  $\beta_D$ , and lattice strain,  $\beta_S$ :  $\beta = \beta_D + \beta_S$ . These are very crude models but still, are useful when comparing samples prepared in a series in which one parameter is varied, for example, calcination time.

To apply some of the models mentioned above, it is necessary to remove the effect of the instrumental broadening from the diffraction peak. This is achieved by measuring  $\beta$  in a polycrystalline sample free of lattice strain and with a very large crystallite size so that all the width of the diffraction peak is because of the instrumental effects. Nowadays, one of the main samples used for this purpose is the reference material LaB<sub>6</sub> (SRM660b) commercialized by the National Institute of Standard Technology – NIST (Black *et al.*, 2010), which can be considered expensive for researchers in developing countries. Other samples can also be used, for example, Courbion and Ferey (1988) synthesized Na<sub>2</sub>Ca<sub>3</sub>Al<sub>2</sub>F<sub>14</sub> (not certified by NIST) that was used by Gozzo *et al.* (2006) to remove the instrumental width of a synchrotron source obtaining the smallest intrinsic width known by the authors.

In this work, the authors present a co-precipitation synthesis route combined with a calcination step at a high temperature to obtain polycrystalline CeO<sub>2</sub> suitable for use as a line width reference sample. The authors show that the diffraction patterns of the CeO<sub>2</sub> samples prepared with this route have diffraction peak widths as sharp as the LaB<sub>6</sub>, and therefore can substitute the latter as a line profile reference material. This route has the advantage of being simple and less expensive than to acquire the SRM660b.

<sup>a)</sup> Author to whom correspondence should be addressed. Electronic mail: andersondmlb@gmail.com

## II. EXPERIMENTAL

### A. Specimen preparation

The cerium oxide ( $\text{CeO}_2$ ) samples were synthesized by first dissolving 15 g of cerium sulfate tetra-hydrate ( $\text{Ce}[\text{SO}_4]_2 \cdot 4\text{H}_2\text{O}$ ), reagent from Sigma Aldrich with purity >98%, in 100 ml of distilled water at room temperature. This solution was kept under constant agitation using a magnetic stirrer and at the end of 15 min, the cerium sulfate was completely dissolved. Second, 25 ml of ammonium hydroxide ( $\text{NH}_4\text{OH}$ ), reagent from Dinâmica with 26%  $\text{NH}_3$ , was slowly added to this solution. During this process, which took 20 min, the solution was also kept under constant agitation. The result was the formation of a precipitate. Third, this mixture was placed on a Falcon<sup>®</sup> tube and centrifuged at 1500 r.p.m. (25 Hz) for 5 min and the supernatant was removed. Distilled water was added to the Falcon<sup>®</sup> tube and the mixture was centrifuged again. This washing process was repeated six times. A sample of this precipitate was dried at 100 °C and X-ray powder diffraction measurements showed it was nanocrystalline  $\text{CeO}_2$ . Audebrand *et al.* (2000) used a similar route to obtain  $\text{CeO}_2$  nanoparticles. It is believed that the mixture of cerium (IV) sulfate and ammonium hydroxide creates a hydrous oxide  $\text{CeO}_2 \cdot x\text{H}_2\text{O}$  which decomposes to  $\text{CeO}_2$  (Audebrand *et al.*, 2000; Tok *et al.*, 2007).

Fourth, the precipitate was added to 25 ml of an aqueous solution containing 20% of hydrogen peroxide and kept under agitation for 60 min using a magnetic stirrer, for cleaning purposes, removing any organic impurities (Mikutta *et al.*, 2005). This step does not interfere with the  $\text{CeO}_2$ . This mixture of  $\text{CeO}_2$  and water was taken to a furnace to dry at 100 °C and the resulting powder was ground in an agate mortar.

X-ray powder diffraction measurements showed very broad peaks indicating that the powder was formed of nanoparticles. The nanoparticles were exposed to air and did not present apparent instability. However, the authors recommend the specimen to be stored in a manner to avoid humidity. This powder was then calcined at 1200 °C for 48 h in a rotary tube furnace for particle growth (Braga *et al.*, 2015; Guimarães *et al.*, 2015). Two heating rates were tested in the calcination step, 5 and 15 °C  $\text{min}^{-1}$ . Figure 1 shows the summary of these steps.

### B. Experimental methods

The X-ray powder diffraction measurements were done on a laboratory setup and at a synchrotron facility. The laboratory setup was a Xpert Pro MPD – PANalytical diffractometer, using  $\text{CoK}\alpha$  ( $\lambda = 1.7889 \text{ \AA}$ ) radiation at 40 kV and 40 mA in parallel beam geometry using a hybrid monochromator composed of one mirror and two Ge (220) crystals.

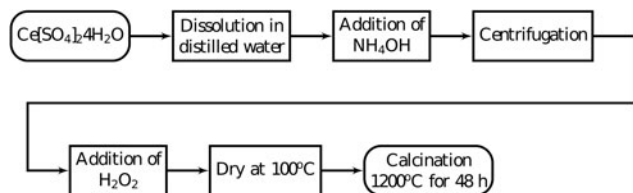


Figure 1. Co-precipitation synthesis steps to synthesize cerium oxide to use as a reference material for X-ray diffraction peak widths.

The height of the X-ray beam emerging from the hybrid monochromator was 1.2 mm. Divergence slits of  $1/8^\circ$  and diffracted beam Soller slits of 0.02 rad were used to control axial divergence. The full width at half maximum of the Si(111) reflection of a Si single crystal reference sample was approximately  $0.0068^\circ$ . The diffraction patterns were obtained from  $2\theta = 20^\circ$  to  $120^\circ$  with steps of  $0.013^\circ$  in 150 min. The specimen in this diffractometer was prepared over a zero-background silicon plate with a diameter of 25 and 2 mm thickness, containing a cavity with a diameter of 10 mm and depth of 0.2 mm.

High-resolution synchrotron powder diffraction data were collected using beamline 11-BM at the Advanced Photon Source, Argonne National Laboratory using an average wavelength of 0.41 Å. Discrete detectors covering an angular range from 6 to  $16^\circ 2\theta$  are scanned over a  $34^\circ 2\theta$  range, with data points collected every  $0.001^\circ 2\theta$  and scan speed of  $0.01^\circ/\text{s}$ . The beam divergence at 30 keV was  $0.005^\circ$  (Wang *et al.*, 2008). A Kapton capillary of the inner diameter of 0.8 mm was filled with 8 to 10 mm of the sample and closed in both extremities with play dough.

The full width at half maximum was obtained by fitting the diffraction peaks with a Split-pseudoVoigt function. This function has two parameters for peak width, one for each side of the peak, so that it can try to account for asymmetry.

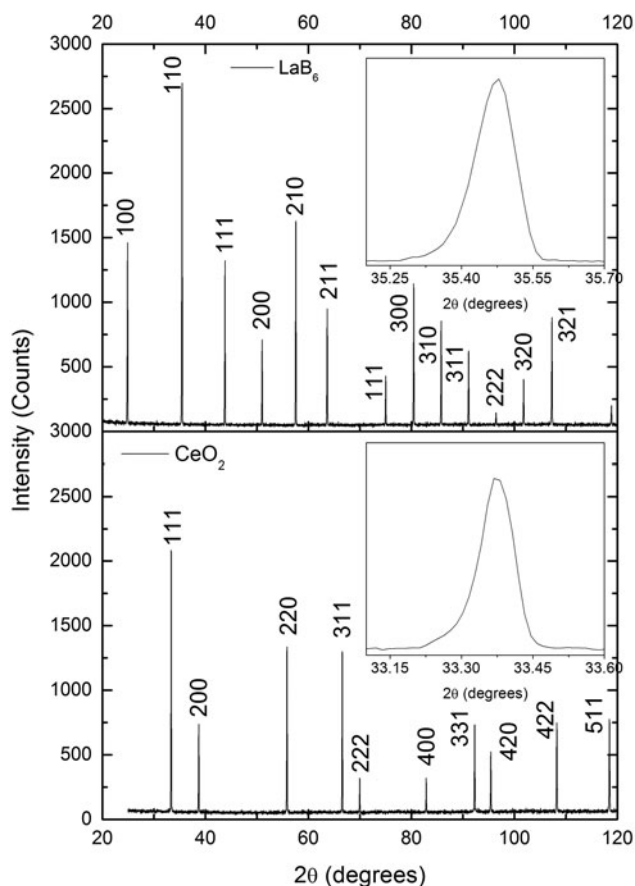


Figure 2. Comparison of the X-ray powder diffraction patterns of one  $\text{CeO}_2$  sample prepared in this work and  $\text{LaB}_6$  supplied by NIST. The peak widths of both patterns are very similar, which suggests that the  $\text{CeO}_2$  sample is composed of large crystallites with negligible strain, just like  $\text{LaB}_6$ . The diffraction patterns were obtained under the same conditions in a parallel beam laboratory diffractometer.

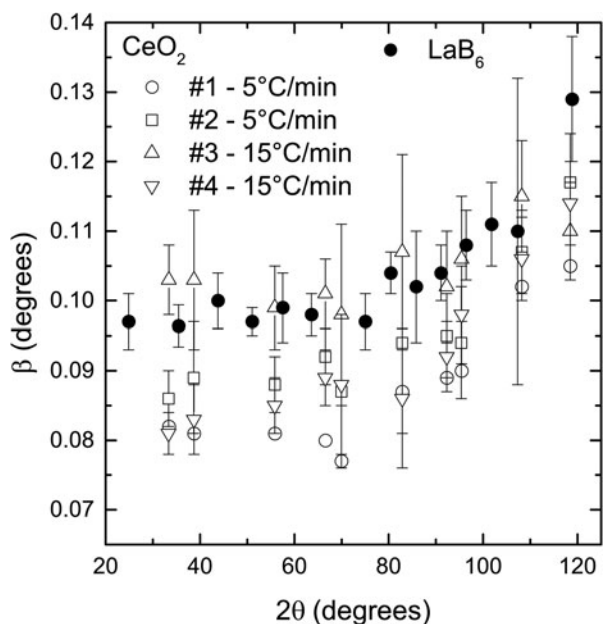


Figure 3. Comparison of the diffraction peak widths of the CeO<sub>2</sub> samples prepared using two heating rates and LaB<sub>6</sub> supplied by NIST. The spread in peak widths of the samples prepared under the same conditions is larger than any supposed difference caused by the heating rate. The widths of all CeO<sub>2</sub> samples are smaller or slightly larger with the widths of LaB<sub>6</sub>. The powder diffraction patterns were obtained under the same conditions in a parallel beam laboratory diffractometer.

The software used for this purpose was the Xpert High Score from PANalytical (Degen *et al.*, 2014).

The micrographs were obtained in a TM-3000 Hitachi scanning electron microscope using 30 000× magnification and operating at 15 kV.

### III. RESULTS AND DISCUSSION

The diffraction patterns of the CeO<sub>2</sub> samples prepared in this work and the LaB<sub>6</sub> sample produced by the NIST are very similar when peak widths are compared (Figure 2). Because these widths are a measure of crystallite size and lattice strain, these results suggest that the CeO<sub>2</sub> samples are composed of large crystallites with negligible lattice strain, just like the LaB<sub>6</sub>.

Two sets of samples were prepared with different heating rates, namely 5 °C/min and 15 °C/min<sup>-1</sup>, to test their effect on the widths of the diffraction peaks. It is supposed that the heating rate determines the speed that the nanoparticles fuse to form larger particles. A slow rate would favor growth by allowing more time for neighbor particles to coalesce, giving rise to large particles and small peak widths. On the other hand, a fast rate could introduce defects on the crystalline structure by not allowing enough time for the atoms to accommodate in the crystallite boundary and release the stress, which would result in large peak widths.

The spread in peak widths of the CeO<sub>2</sub> samples prepared under the same conditions is larger than a supposed difference in widths caused by the heating rate (Figure 3). For example, sample #1, prepared with 5 °C/min<sup>-1</sup>, has smaller peak widths than the two samples prepared with 15 °C/min<sup>-1</sup> (#3, #4). However, sample #2, which was also prepared with 5 °C/min<sup>-1</sup>, has peak with values between samples #3 and #4.

Despite this intrinsic spread in peak widths produced by the synthesis route presented in this work, in general, the peak widths of the CeO<sub>2</sub> samples are smaller or slightly larger than the peak widths of the LaB<sub>6</sub> (Figure 3). Because the peak widths are the most relevant features of a reference material used to remove instrumental broadening, CeO<sub>2</sub> samples

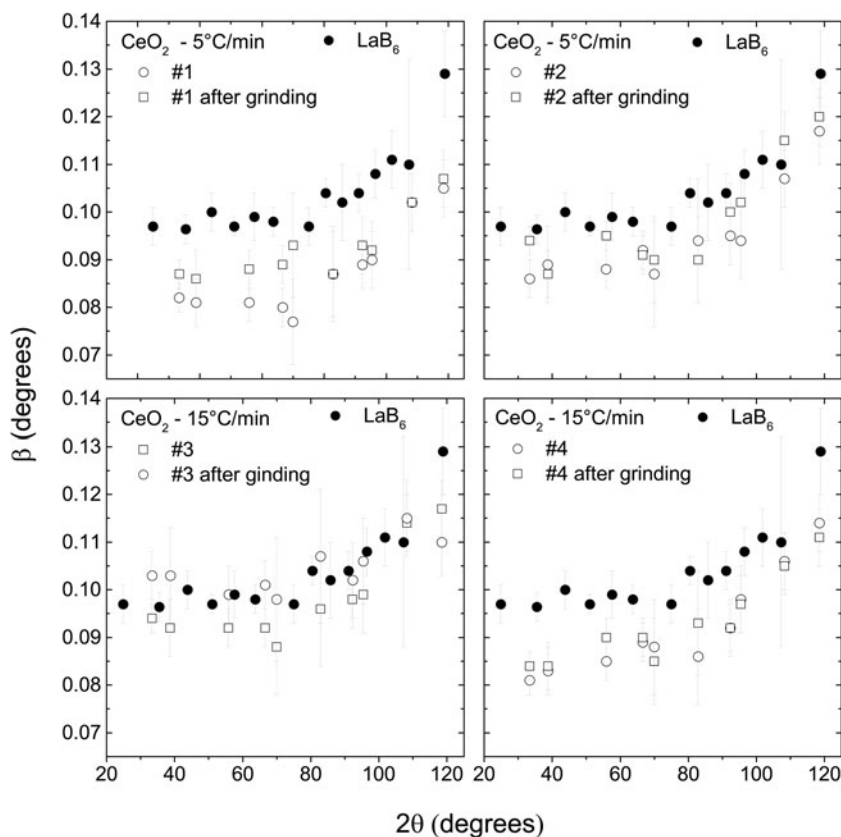


Figure 4. The widths of the diffraction peaks of the CeO<sub>2</sub> samples increase after they are ground. Nevertheless, they are still smaller than the widths of the LaB<sub>6</sub>. The powder diffraction patterns were obtained under the same conditions in a parallel beam laboratory diffractometer.



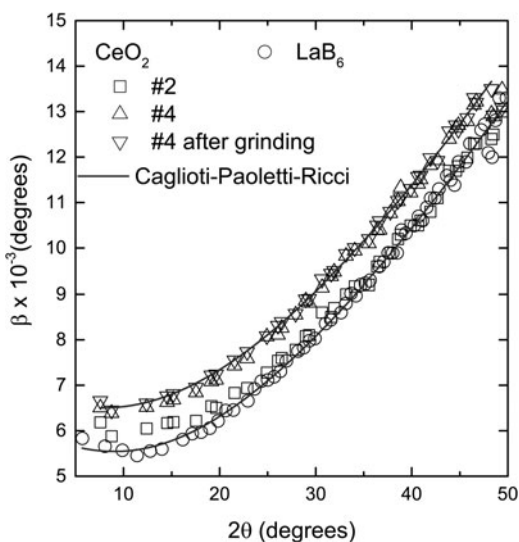


Figure 5. Comparison of the diffraction peak widths of the  $\text{CeO}_2$  and  $\text{LaB}_6$  obtained in a high-resolution synchrotron facility. The widths of sample #2 are almost the same as the widths of  $\text{LaB}_6$ , and smaller than #4 by approximately  $0.001^\circ$ . Grinding has a negligible effect on the widths. The points for each sample follow a typical Caglioti–Paoletti–Ricci (1958) curve with  $U = 9.66 \pm 0.28 \times 10^{-4}$ ,  $V = -1.54 \pm 0.14 \times 10^{-4}$  and  $W = 3.68 \pm 0.16 \times 10^{-5}$  for  $\text{LaB}_6$  and #2, and  $U = 8.94 \pm 0.46 \times 10^{-4}$ ,  $V = -9.23 \pm 0.23 \times 10^{-5}$  and  $W = 4.32 \pm 0.27 \times 10^{-5}$  for #4. The error bars are, in average, of the size of the points and were omitted for better visualization.

prepared following the synthesis route shown in this work can be used instead of  $\text{LaB}_6$ .

The  $\text{CeO}_2$  samples were also ground to test the effect of this treatment on the peak widths. A finer powder with a sharp particle distribution delivered by the grinding process is easier to mount for X-ray powder diffraction measurements and prevents surface roughness and preferred orientations. On the other hand, it is believed that grinding could induce micro strain in the crystalline structure, which in turn broadens the diffraction peaks. Another possibility is that the crystallites are broken in the process, also resulting in broader peaks.

The peak widths of the  $\text{CeO}_2$  samples increase after they were ground (Figure 4), suggesting that some lattice strain is introduced and/or average crystallite size is reduced. Nevertheless, the peak widths are still smaller or very slightly larger than the peak widths of  $\text{LaB}_6$ . Therefore, these ground samples could also be used to substitute  $\text{LaB}_6$  for removing instrumental width.

The widths of the diffraction peaks of the  $\text{LaB}_6$  and  $\text{CeO}_2$  samples, obtained in a high-resolution synchrotron instrument, are only slightly different,  $<0.001^\circ$  (Figure 5). Because the instrument contribution to the widths of the diffraction peaks in this apparatus is a lot less than in a conventional diffractometer, it is easier to detect the contribution of the crystallite size and/or lattice strain of the sample. Sample #2 and  $\text{LaB}_6$  have practically the same widths while #4 has slightly larger ones. This confirms that the contributions of size and lattice strain of  $\text{CeO}_2$  to the peak widths are similar to the contributions of  $\text{LaB}_6$ , therefore these samples can be used to remove instrumental broadening.

The cerium samples were also characterized morphologically using scanning electron microscopy. Figure 6 shows the micrographs of  $\text{LaB}_6$  (A) and  $\text{CeO}_2$   $15^\circ\text{C}/\text{min}^{-1}$  (B). Both samples are composed of particles roughly in the range between 1 and  $5\ \mu\text{m}$ . The  $\text{CeO}_2$  also presents large particles of about  $10\ \mu\text{m}$  (not shown here), which are probably generated by the coalescence of smaller particles. Nevertheless, even with the presence of large and small particles (crystallite size distribution) probably lattice strain as well, this sample is comparable with the  $\text{LaB}_6$  because it provides slightly smaller diffraction peak widths. The presence of small and large particles in the  $\text{CeO}_2$  may be an issue if one tries to use this sample as a standard for a purpose other than to obtain the instrumental widths, for example, the large spread in particle distribution introduces preferred orientation effects which must not happen in an intensity standard (Langford and Louër, 1996). Nevertheless, this effect does not compromise the diffraction peak widths and therefore does not diminish the capacity of the sample for removing diffraction peak instrumental broadening.

#### IV. CONCLUSION

The authors have presented a simple synthesis route, based on co-precipitation, to obtain micron size polycrystalline  $\text{CeO}_2$  powder to be used as an X-ray diffraction peak width reference material. The full width at half maximum of the  $\text{CeO}_2$  diffraction peaks is as small as the one of the  $\text{LaB}_6$  SRM660b supplied by NIST, indicating they represent the instrumental breadth of the 11-BM beamline, being free from sample effects. For the parallel beam laboratory diffractometer, the difference in full width at half maximum of the two samples is larger and possibly caused by sample mounting and absorption. In addition, the  $\text{CeO}_2$  samples are less expensive than the SRM660b.

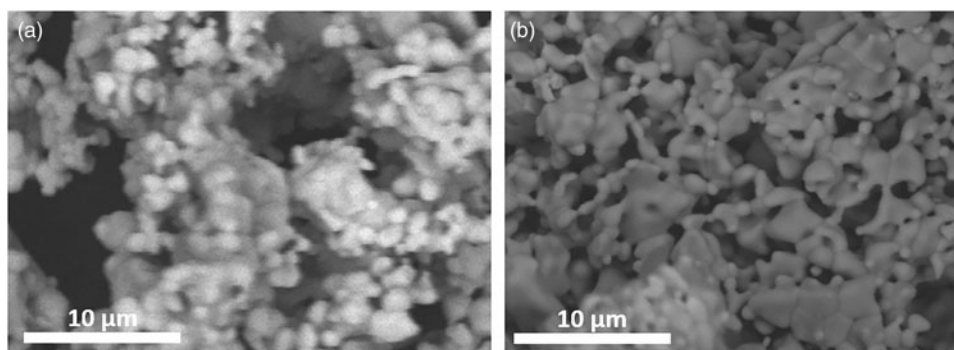


Figure 6. Scanning electron microscope images of (a)  $\text{LaB}_6$  (SRM660b) and (b)  $\text{CeO}_2$ .

## ACKNOWLEDGEMENTS

J. M. Sasaki would like to thank the Conselho Nacional de Desenvolvimento Científico e Tecnológico - CNPq/Brazil for his research fellowship under grant number 3063692014-1. A. M. L. Batista and M. A. R. Miranda would like to thank Fundação Cearense de Apoio ao Desenvolvimento Científico e Tecnológico – FUNCAP/Brazil for their graduate scholarship. Use of the Advanced Photon Source at Argonne National Laboratory was supported by the U. S. Department of Energy, Office of Science, Office of Basic Energy Sciences, under Contract No. DE-AC02-06CH11357.

- Audebrand, N., Auffrédic, J. and Louër, D. (2000). "An X-ray powder diffraction study of the microstructure and growth kinetics of nanoscale crystallites obtained from hydrated cerium oxides," *Chem. Mater.*, **12**, 1791–1799.
- Azároff, L. V. and Buerger, M. J. (1958). *The Powder Method in X-ray Crystallography* (McGraw-Hill, New York).
- Black, D. R., Windover, D., Henins, A., Filliben, J. and Cline, J. P. (2010). "Standard reference material 660b for X-ray metrology," in Denver X-ray conference on Applications of X-ray Analysis, vol. **54**, pp. 140–148.
- Braga, T. P., Dias, D. F., Sousa, M. F., Soares, J. M. and Sasaki, J. M. (2015). "Synthesis of a fair stable FeCo alloy nanocrystallite by proteic sol-gel method using a rotary oven," *J. Alloys Compd.* **622**, 408–417.
- Burton, A. W., Ong, K., Rea, T. and Chan, I. Y. (2009). "On the estimation of average crystallite size of zeolites from the Scherrer equation: a critical evaluation of its application to zeolites with one-dimensional pore systems," *Microporous Mesoporous Mater.* **117**, 75–90.
- Caglioti, G., Paoletti, A., Ricci, F. P. (1958). "Choice of collimators for a crystal spectrometer for neutron diffraction," *Nuclear Instrum.* **3**, issue (4), 223–228.
- Cervellino, A., Frison, R., Bertolotti, F. and Guagliardi, A. (2015). "DEBUSSY 2.0: the new release of a Debye user system for nanocrystalline and/or disordered materials," *J. Appl. Cryst.* **48**, 2026–2032.
- Courbion, G. and Ferey, G. (1988). "Na<sub>2</sub>Ca<sub>3</sub>Al<sub>2</sub>F<sub>14</sub>: Aa new example of a structure with "independent F" – Aa new method of comparison between fluorides and oxides of different formula," *J. Solid State Chem.* **76**, 426–431.
- Degen, T., Sadki, M., Bron, E., König, U. and Nénert, G. (2014). "The high-score suite," *Powder Diffr. Powder Diffr.* **29**, 13–18.
- Gozzo, F., De Caro, L., Giannini, C., Guagliardi, A., Schmitt, B. and Prodi, A. (2006). "The instrumental resolution function of synchrotron radiation powder diffractometers in the presence of focusing optics," *J. Appl. Cryst.* **39**, 347–353.
- Guimarães, G. F., Sasaki, J. M., Sousa, J. P., Miranda, M. A. R., Carvalho, J. A., Menezes, J. W. M., and Oliveira, W. F. (2015) "Aperfeiçoamento introduzido em equipamento de estágio de rotação aplicado em forno tubular". Brazil patent BR 10 2015 031518 0.
- Hall, W. H. (1949). "X-Ray line broadening in metals," *Proc. Phys. Soc. A.* **62**, 741–743.
- Holzwarth, U. and Gibson, N. (2011). "The Scherrer equation versus the 'Debye-Scherrer equation'," *Nat. Nanotech.* **6**, 534.
- James, R. W. (1962). *The Optical Principles of the Diffraction of X-Rays, Volume II of The Crystalline State* (G Bell and Sons Ltda, London).
- Klug, P. and Alexander, L. E. (1974). *X-Ray Diffraction Procedures for Polycrystalline and Amorphous Materials* (Wiley, New York).
- Langford, J. I. and Louër, D. (1996). "Powder diffraction," *Rep. Prog. Phys.* **59**, 131–234.
- Langford, J. I. and Wilson, A. J. C. (1978). "Scherrer after sixty years: a survey and some new results in the determination of crystallite size," *J. Appl. Cryst.* **11**, 102–113.
- Mikutta, R., Kleber, M., Kaiser, K., Jahn, R. (2005). "Review: organic matter removal from soils using hydrogen peroxide, sodium hypochlorite, and disodium peroxodisulfate," *Soil Sci. Soc. Am. J.*, **69**, 120–135.
- Patterson, A. L. (1939). "The Scherrer formula for X-ray particle size determination," *Phys. Rev.* **56**, 978–982.
- Scardi, P., Ortolani, M. and Leoni, M. (2010). "WPPM: microstructural analysis beyond the Rietveld Method," *Mater. Sci. Forum.* **651**, 155–171.
- Tok, A. I. Y., Boey, F. Y. C., Dong, Z. and Sun, X. L. (2007) "Hydrothermal synthesis of CeO<sub>2</sub> nano-particles," *J. Mater. Process. Technol. Journal of Materials Processing Technology*, **190**, 217–222.
- Vives, S., Gaffet, E. and Meunier, C. (2004). "X-ray diffraction line profile analysis of iron ball milled powders," *Mater. Sci. Eng., A.* **366**, 229–238.
- Wang, J., Toby, B. H., Lee, P. L., Ribaud, L., Antao, S. M., Kurtz, C., Ramanathan, M., Von Dreele, R. B. and Beno, M. A. (2008). "A dedicated powder diffraction beam line at the Advanced Photon Source: commissioning and early operational results," *Rev. Sci. Instrum.*, **79**, 1–7.
- Warren, B. E. and Averbach, B. L. (1950). "The effect of Cold-Work distortion on X-ray patterns," *J. Appl. Phys.* **21**, 595–599.
- Williamson, G. K. and Hall, W. H. (1953). "X-Ray line broadening from filed aluminum and wolfram," *Acta Metall. Acta Metall.* **1**, 22–31.